Cancer Cell
Article

Tet2 Loss Leads to Increased Hematopoietic Stem Cell Self-Renewal and Myeloid Transformation

Kelly Moran-Crusio,[1,2,11] Linsey Reavie,[1,2,11] Alan Shih,[3,4,11] Omar Abdel-Wahab,[3,4] Delphine Ndiaye-Lobry,[1,2] Camille Lobry,[1,2] Maria E. Figueroa,[5] Aparna Vasanthakumar,[6] Jay Patel,[3] Xinyang Zhao,[7] Fabiana Perna,[7] Suveg Pandey,[3] Jozef Madzo,[6] Chunxiao Song,[8] Qing Dai,[8] Chuan He,[8] Sherif Ibrahim,[1] Miloslav Beran,[9] Jiri Zavadil,[10] Stephen D. Nimer,[4,7] Ari Melnick,[5] Lucy A. Godley,[6] Iannis Aifantis,[1,2,11,*] and Ross L. Levine[3,4,11,*]
[1]Department of Pathology and NYU Cancer Institute
[2]Howard Hughes Medical Institute
New York University School of Medicine, New York, NY 10016, USA
[3]Human Oncology and Pathogenesis Program
[4]Leukemia Service, Department of Medicine
Memorial Sloan-Kettering Cancer, New York, NY 10016, USA
[5]Division of Hematology/Oncology, Weill Cornell Medical College, New York, NY 10016, USA
[6]Department of Medicine, The University of Chicago, Chicago, IL 60637, USA
[7]Molecular Pharmacology and Chemistry Program, Sloan-Kettering Institute, New York, NY 10016, USA
[8]Department of Chemistry and Institute for Biophysical Dynamics, The University of Chicago, Chicago, IL 60637, USA
[9]Department of Leukemia, M.D. Anderson Medical Center, Houston, TX 77030, USA
[10]Department of Pathology, NYU Cancer Institute and Center for Health Informatics and Bioinformatics, NYU Langone Medical Center, New York, NY 10016, USA
[11]These authors contributed equally to this work
*Correspondence: iannis.aifantis@nyumc.org (I.A.), leviner@mskcc.org (R.L.L.)
DOI 10.1016/j.ccr.2011.06.001

SUMMARY

Somatic loss-of-function mutations in the ten-eleven translocation 2 (*TET2*) gene occur in a significant proportion of patients with myeloid malignancies. Although there are extensive genetic data implicating *TET2* mutations in myeloid transformation, the consequences of Tet2 loss in hematopoietic development have not been delineated. We report here an animal model of conditional *Tet2* loss in the hematopoietic compartment that leads to increased stem cell self-renewal in vivo as assessed by competitive transplant assays. *Tet2* loss leads to a progressive enlargement of the hematopoietic stem cell compartment and eventual myeloproliferation in vivo, including splenomegaly, monocytosis, and extramedullary hematopoiesis. In addition, *Tet2*$^{+/-}$ mice also displayed increased stem cell self-renewal and extramedullary hematopoiesis, suggesting that *Tet2* haploinsufficiency contributes to hematopoietic transformation in vivo.

INTRODUCTION

Genetic studies of patients with myeloid malignancies have identified recurrent somatic alterations in the majority of patients with myeloproliferative neoplasms (MPNs), myelodysplastic syndromes (MDSs), and acute myeloid leukemia (AML). A subset of myeloid disease alleles can be classified into two distinct complementation groups: one class that includes mutations that activate oncogenic signaling pathways, and a second class of mutations that perturbs myeloid differentiation (Gilliland and Griffin, 2002). However, recent studies have suggested that this model of myeloid transformation does not accurately represent the biologic and clinical heterogeneity of MPN, MDS, and AML, and that not all leukemogenic disease alleles can be

Significance

Recurrent somatic mutations in *TET2* and in other genes that regulate the epigenetic state have been identified in patients with myeloid malignancies and in other cancers. However, the effects of *Tet2* loss have not yet been studied in an in vivo model. We report here that *Tet2* loss leads to increased stem cell self-renewal and to progressive stem cell expansion. Consistent with human mutational data, *Tet2* loss leads to myeloproliferation in vivo, notable for splenomegaly and monocytic proliferation. In addition, haploinsufficiency for Tet2 confers increased self-renewal and myeloproliferation, suggesting that the monoallelic TET2 mutations found in most patients can contribute to myeloid transformation. This work demonstrates that reduction in TET2 expression or function leads to enhanced stem cell function in vivo and myeloid transformation.

classified by their ability to directly affect signaling and/or differentiation. Consonant with this notion, recent studies have identified recurrent mutations of known and putative epigenetic modifiers in patients with myeloid malignancies. These include somatic mutations in chromatin-modifying enzymes (Ernst et al., 2010; Nikoloski et al., 2010) and in DNA methyltransferases (Ley et al., 2010; Yamashita et al., 2010). In addition, biologic studies of recurrent chromosomal translocations, including MLL fusions, have shown that leukemogenic fusion proteins alter epigenetic regulation in hematopoietic cells, resulting in changes in chromatin state at specific loci (Dorrance et al., 2006; Krivtsov et al., 2008). Taken together, these data suggest that somatic alterations in genes that regulate the epigenetic state of hematopoietic cells are a common pathogenetic event in leukemogenesis (Abdel-Wahab and Levine, 2010). Importantly, recent studies have identified recurrent mutations in epigenetic master regulators in lymphoid malignancies (Morin et al., 2010) and in solid tumors (van Haaften et al., 2009; Varela et al., 2011), suggesting that mutational dysregulation of the epigenetic machinery is a common theme in oncogenic transformation.

Recent studies have identified a novel class of somatic mutations in myeloid malignancies. Specifically, somatic deletions and loss-of-function mutations in the ten-eleven translocation 2 (*TET2*) gene were identified in 10%–20% of patients with MDS and MPN (Delhommeau et al., 2009; Langemeijer et al., 2009); subsequent studies identified recurrent *TET2* mutations in patients with chronic myelomonocytic leukemia (CMML) and AML (Abdel-Wahab et al., 2009; Jankowska et al., 2009), and demonstrated that *TET2* mutations were associated with adverse outcome in intermediate-risk AML (Metzeler et al., 2011). Within the TET family of proteins, TET1, TET2, and TET3 have been shown to modify DNA by hydroxylating 5-methylcytosine (5mC) (Ko et al., 2010; Tahiliani et al., 2009), and the TET2 mutant proteins observed in these patients with myeloid malignancies have been shown to be deficient in this enzymatic function (Ko et al., 2010). In addition, recent work demonstrated that mutations in the metabolic enzymes IDH1 and IDH2 (Mardis et al., 2009; Parsons et al., 2008; Ward et al., 2010; Yan et al., 2009) are mutually exclusive with *TET2* mutations, and that production of 2-hydroxyglutarate by neomorphic IDH1/2 mutant proteins (Dang et al., 2009) inhibits TET2 catalytic activity (Figueroa et al., 2010; Xu et al., 2011). Taken together, these data indicate that mutations that impair 5-hydroxymethylation represent a novel mechanism of transformation in myeloid malignancies.

Although there are extensive genetic data implicating *TET2* mutations in myeloid transformation, the consequences of Tet2 loss in hematopoietic development have not been delineated. Recent in vitro studies using shRNA-based approaches have suggested a role for TET2 in regulating myeloid differentiation (Figueroa et al., 2010; Ko et al., 2010) and in regulating stem/progenitor cell proliferation (Figueroa et al., 2010). In order to elucidate the function of *Tet2* in hematopoiesis in vivo, we describe here the characterization of conditional deletion of *Tet2* in the hematopoietic compartment demonstrating a role for *Tet2* in regulating hematopoietic stem cell renewal and differentiation. These findings provide a model for human disease in which the loss of *Tet2*, often through the loss of a single allele, leads to increased self-renewal and myeloid transformation, and provides insight into how mutations in epigenetic modifiers contribute to malignant transformation.

RESULTS

Tet2-Expression Silencing Leads to Increased Replating Capacity

We first investigated the effects of *Tet2* silencing in hematopoiesis by transducing whole mouse bone marrow cells with retroviral vectors encoding validated *Tet2* shRNA vectors (Figueroa et al., 2010), and sorting for GFP-positive cells. Stable shRNA-mediated knockdown led to stable reductions in TET2 expression by 50%–70% (Figure 1A). Because TET2 is an enzyme that hydroxylates 5mC on DNA, its knockdown should lead to loss of 5-hydroxylation of methylcytosine (5hmC). We used a mass spectrometry-based approach (Shah et al., 2010) to demonstrate that *Tet2* silencing results in a significant reduction in 5hmC in GFP^+ hematopoietic cells stably expressing *Tet2* shRNAs (Figure 1B). GFP^+ cells were then plated in methylcellulose for CFU in vitro assays. We observed no significant differences in the number or the lineage specificity of *Tet2*-expressing and *Tet2*-silenced colonies after the first plating. However, at the second plating there was a 2-fold increase in the number of colonies expressing *Tet2*-specific shRNAs (Figure 1C). Strikingly, *Tet2*-silenced cells retained the ability to serially replate and generate colonies, although essentially no wild-type colonies were detected after the second plating. In agreement with the putative acquisition of a more immature phenotype, *Tet2* shRNA-expressing colonies upregulated c-Kit, a hematopoietic stem and progenitor cell marker (Figure 1D). These initial studies demonstrated that *Tet2* silencing reduces global 5hmC levels and increases the replating capacity of hematopoietic stem and progenitor cells.

Generation of a Conditional *Tet2* Knockout Allele

Although these studies provide important information on TET2 function, hematopoiesis is a dynamic process that is most accurately studied in vivo. Thus, we decided to conditionally inhibit *Tet2* gene expression in the hematopoietic compartment. We first assessed *Tet2* expression by performing qRT-PCR of sorted hematopoietic stem/progenitor subsets (LSK: Lin^- $Sca\text{-}1^+$ $c\text{-}Kit^+$; common myeloid progenitor [CMP]: Lin^- $Sca\text{-}1^-c\text{-}Kit^+$, $Fc\gamma R^{lo}$ $CD34^+$; GMP: Lin^- $Sca1^-$ $c\text{-}Kit^+$ $Fc\gamma R^+CD34^+$, MEP: Lin^- $Sca\text{-}1^-$ $c\text{-}Kit^+$ $Fc\gamma R^-CD34^-$) and in differentiated hematopoietic lineages. Expression studies revealed that *Tet2* expression was ubiquitously expressed in the hematopoietic compartment, including in stem and progenitor subsets and in mature myeloid and lymphoid cells (Figure 2A). Purified human $CD34^+$ peripheral blood-mobilized cells also demonstrated expression of *TET2* in human hematopoietic stem cells (see Figure S1A available online). Two different *TET2* isoforms are expressed, including a shorter isoform b that lacks the C-terminal enzymatic domain. To understand the nature and location of *TET2* mutations in human myeloid malignancies and how this would inform our mouse model, we analyzed *TET2* mutations from 991 patients with a variety of myeloid malignancies (MPN, CMML, and AML). Exon 3 in the murine *Tet2* locus encodes for approximately half of the TET2 protein; analysis from the mutational data identifies the corresponding exon 3 of human *TET2* as the

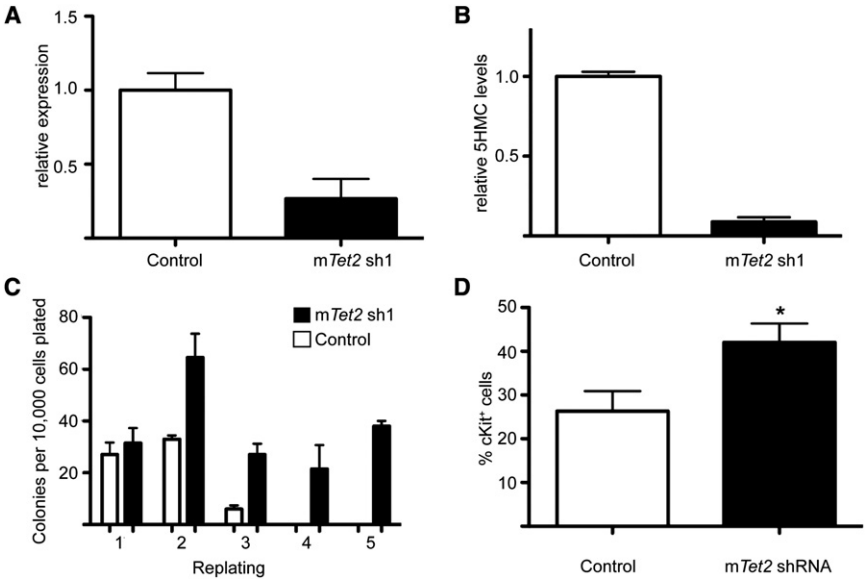

Figure 1. In Vitro *Tet2*-Expression Silencing Leads to Increased Serial Replating

(A) Quantification of the shRNA-mediated *Tet2* knockdown efficiency using qRT-PCR.

(B) Quantification of 5hmC by LC/MS of control (MSCV-IRES-GFP) versus Tet2 knockdown-derived cells after retroviral transduction and GFP sorting.

(C) CFU assay of bone marrow-derived cells infected with control or *Tet2* shRNA virus. Colony counts were scored every 14 days.

(D) Upregulation of surface c-Kit expression in progenitors expressing *Tet2*-specific shRNA. *$p < 0.026$. Error bars represent ± SD.

most frequently mutated exon in myeloid malignancies, including a large number of nonsense mutations, insertions, and deletion mutations that truncate the protein. Specifically, we found that 41.5% (51 of 123) of *TET2* mutations occurred in the first coding exon of *TET2* (exon 3), whereas 29.3% (36 of 123) of *TET2* mutations occurred in the last coding exon (exon 11) (Abdel-Wahab et al., 2009; Figueroa et al., 2010) (Figure 2B; Figure S1B). Moreover, the largest proportion of mutations that results in a premature stop codon occurs in exon 3 (Figure 2B). In addition, exon 3 of *Tet2* is contained within the two described *Tet2* transcripts (*Tet2a* and *Tet2b*), which are both expressed in the hematopoietic compartment (Figure S1A). Therefore, we decided to target exon 3 using homologous recombination. We utilized ES cell targeting to insert two LoxP sites flanking exon 3, as well as an Frt-flanked neomycin selection cassette in the upstream intron (Figure 2C). The generated mice ($Tet2^{f/f}$) were initially crossed to a germline Flp-deleter murine line to eliminate the neomycin cassette, and then subsequently crossed to IFNa-inducible *Mx1-cre*, the hematopoietic-specific *Vav-cre*, and the germline *EIIa-cre* mice (Kühn et al., 1995; Lakso et al., 1996; Stadtfeld and Graf, 2005). Figures 2D and 2E demonstrate the efficient targeting of the locus and the generation of a recombined (E) allele upon Cre recombinase expression in hematopoietic cells. Although *Tet2* was recently suggested to play an important role in ES cell differentiation (Ito et al., 2010; Koh et al., 2011), *EIIa-cre*$^{+}$*Tet2*$^{-/-}$ mice were born with the expected Mendelian ratios with normal growth and organ development. These data suggested that other members of the *Tet* family may have redundant functions in embryonic development and in homeostasis of different tissues. *Vav-Cre*-mediated deletion led to a compete silencing of *Tet2* expression in the bone marrow, thymus, and spleen of *Vav-cre*$^{+}$*Tet2*$^{f/f}$ animals. Interestingly, *Tet2*-expression silencing was not accompanied by changes in expression of either *Tet1* or *Tet3*, which were both expressed in hematopoietic cells at similar levels before and after *Tet2* deletion (Figure 2F).

Tet2 Deletion Leads to an Enhanced Repopulating Capacity of Hematopoietic Progenitors In Vitro

Given that RNAi-mediated *Tet2* silencing led to increased replating potential, we assessed whether deletion of TET2 in different hematopoietic subsets led to similar effects. We performed methylcellulose CFU assays using FACS-sorted Lin^{-}c-Kit^{+} progenitors and LSK CD150^{+} HSC from *Vav-cre*$^{+}$*Tet2*$^{-/-}$ and *Vav-cre*$^{+}$*Tet2*$^{+/+}$ mice. In both cases, *Tet2*-deficient cells demonstrated serial replating capacity (for at least ten replatings followed by continuous liquid culture for 4 additional months), whereas *Tet2*$^{+/+}$ counterparts differentiated and did not generate colonies after the second plating (Figure 3A). *Tet2*$^{-/-}$ colonies were more homogeneous and less differentiated and contained cells with a promyeloblastic morphology (Figure 3B). Indeed, expression of c-Kit, a classical marker of hematopoietic progenitors and the receptor for stem cell factor, was upregulated significantly in *Tet2*$^{-/-}$ and was expressed in nearly all *Tet2*$^{-/-}$ cells in the third plating and beyond (Figure 3C). Furthermore, the c-Kit-expressing cells also upregulated the myeloid progenitor markers CD34 and FcγR (Figure 3C). Interestingly, comparison of gene expression profiles of *Tet2*$^{-/-}$ cells at the fifth plating (CFU5) to different stem and progenitor populations showed that *Tet2*$^{-/-}$ cells share a common gene expression program with CMPs, suggesting that these are indeed c-Kit^{+} myeloid progenitors with the ability to replate indefinitely in culture (Figure S2). *Tet2*$^{-/-}$ myeloid progenitor cells were also characterized by increased expression of the self-renewal regulators *Meis1* and *Evi1*, and by reduced expression of multiple myeloid-specific factors (including *Cebpa*, *Cebpδ*, *Mpo*, and *Csf1*), more consistent with multipotent LSK cells than committed CMP or GMP (Figure S2; data not shown). These findings are consistent with the shRNA knockdown experiments shown in Figure 1 and suggest that *Tet2* loss leads to enhanced serial replating ability in vitro.

Tet2 Deletion Leads to Progressive Defects in Hematopoiesis

We next performed detailed analysis of in vivo hematopoiesis in *Tet2*$^{-/-}$ mice. Detailed phenotypic characterization of young (4–6 weeks) *Vav-Cre*$^{+}$*Tet2*$^{-/-}$ mice failed to reveal gross alterations in bone marrow stem/progenitor numbers or in the

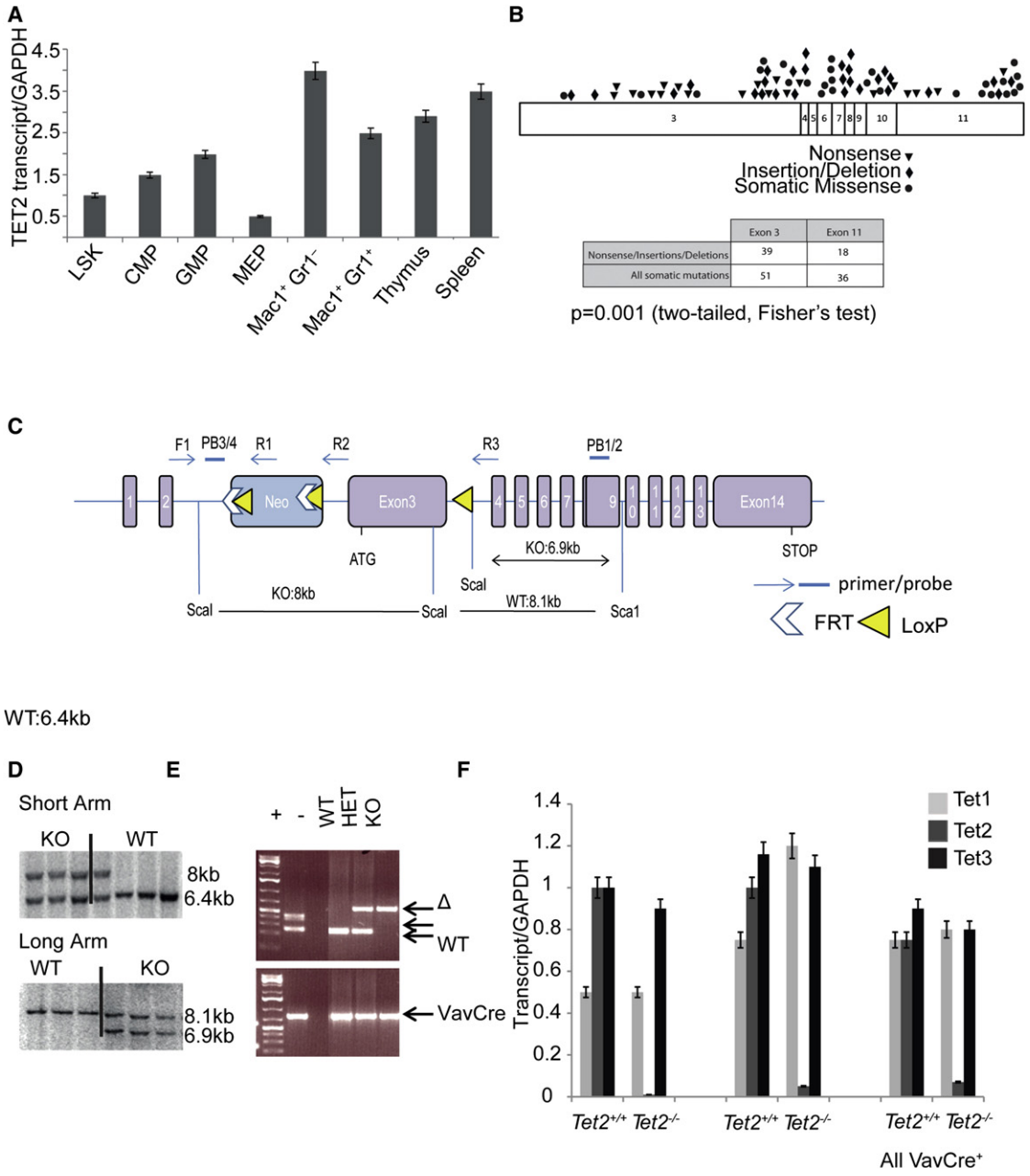

Figure 2. Generation of a Conditional *Tet2* allele

(A) qRT-PCR showing relative expression levels of *Tet2* in purified progenitor and mature mouse hematopoietic stem and progenitor subsets.

(B) Exon distribution of *TET2* mutations found in patients with AML and CMML.

(C) Schematic depiction of the targeted *Tet2* allele. Exon 3 is targeted and flanked by LoxP sites upon Frt-mediated deletion of the NEO cassette.

(D) Verification of correct homologous recombination using Southern blots on targeted ES cells.

(E) Verification of VavCre-mediated excision using genomic PCR. Recombined (Δ), floxed, and wild-type *Tet2* alleles are shown.

(F) Efficiency of *Tet2* knockout using qRT-PCR in purified bone marrow c-Kit$^+$ cells, total thymus, and spleen. Expression of *Tet1* and *Tet3* in wild-type and *Tet2*-deficient bone marrow cells reveals no differences in *Tet1* and *Tet3* expression with *Tet2* deletion. Error bars represent ± SD.

See also Figure S1.

myeloid compartment (Figure 4A, first panel). Likewise, there were no effects on the differentiation of lymphocyte lineages in the bone marrow (data not shown). However, detailed FACS analysis of *Tet2*$^{-/-}$ spleens from young mice identified significant extramedullary hematopoiesis, as defined by a significant increase in the absolute numbers of c-Kit$^+$ (data not shown), LSK cells (including CD150$^+$ HSC), and myeloid progenitors (Figures 4B and 4C). Moreover, purification of *Tet2*$^{+/+}$ and

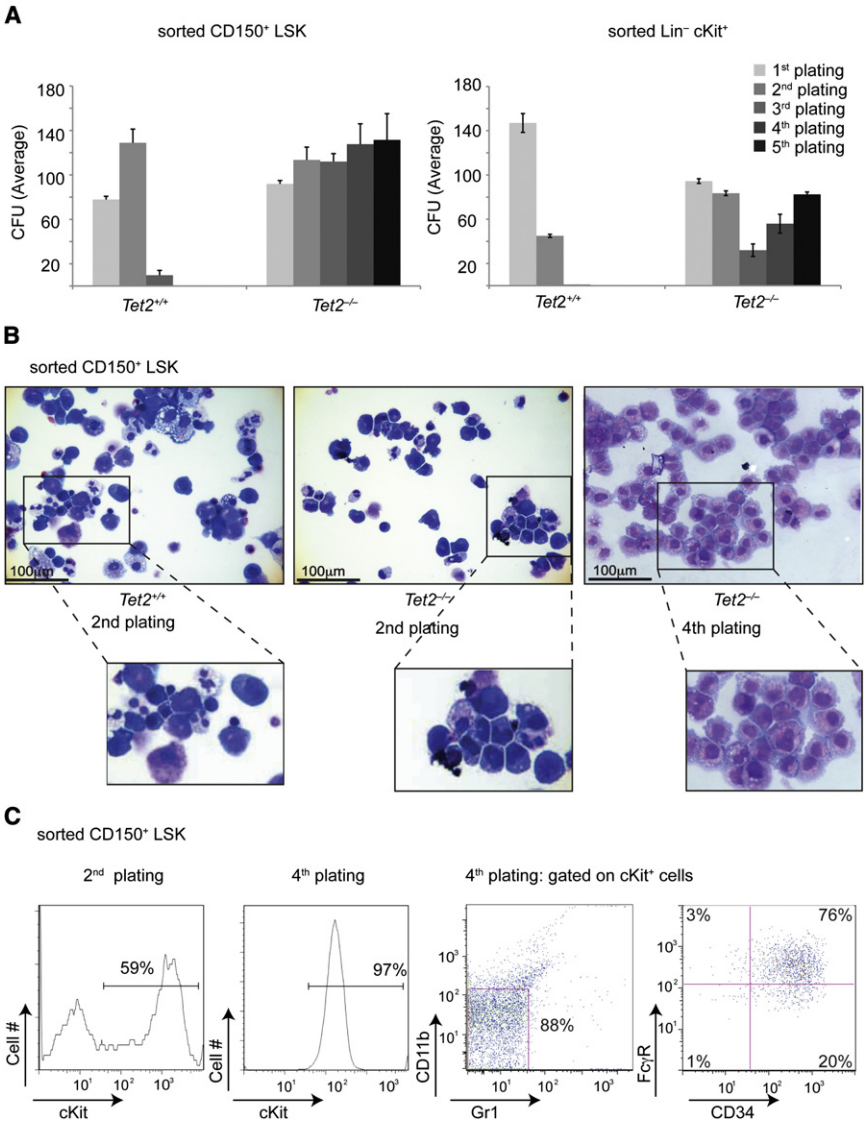

Figure 3. *Tet2* Deficiency Leads to Increased Serial Replating Ability In Vitro

(A) Left panel shows a methylcellulose CFU assay using LSK CD150$^+$-purified cells. Absolute number of colonies is shown at different platings. A similar CFU assay using Lineage$^-$c-Kit$^+$ cells is shown in the right panel.

(B) Morphology of generated colonies either at the 2nd or 4th plating. Cytospins of the colonies are shown.

(C) Left panels illustrate upregulation of surface c-Kit expression at the 2nd and 4th plating. Right panels show cell surface expression of CD34 and FcγR on Lin$^-$cKit$^+$ *Tet2*$^{-/-}$ cells by the 4th plating. A representative example of at least three independent experiments is shown for each assay. Error bars represent ± SD.

See also Figure S2.

Tet2$^{-/-}$ bone marrow progenitor populations (LSK, CMP, GMP) and subsequent transcriptome analysis revealed that *Tet2*$^{-/-}$ LSK cells display a significant enrichment of a CMP gene expression signature (Figure S3; Experimental Procedures), suggesting that *Tet2* loss leads to aberrant hematopoiesis in vivo.

We next analyzed older (20 week) *Tet2*$^{-/-}$ animals to determine the consequences of *Tet2* loss on long-term hematopoiesis. At 20 weeks after *Tet2* deletion, we noted an increase in the size of the bone marrow LSK compartment (Figure 4A, second panel). This phenotype was not accompanied by expansion of a specific stem or multipotential progenitor compartment as defined by the utilization of CD150/CD48 marker labeling. Further analysis of the progenitor compartment showed a marked increase in the GMP population, which includes progenitors of monocytes and granulocytes (Figure 4A). However, the most striking effects of *Tet2* deletion were noted in the spleen of these animals; *Tet2*$^{-/-}$ but not *Tet2*$^{+/+}$ mice displayed splenomegaly at 20 weeks of age, which was associated with an increase in the proportion of total CD11b$^+$ cells (see below). Notably, extramedullary hematopoiesis was prominent, with a significant increase in the absolute number of LSK (Figures 4B and 4C) as well as CD150$^+$ HSC (not shown) cells. These combined studies suggested that *Tet2* deletion leads to progressive defects in blood differentiation and to a significant elevation of extramedullary hematopoiesis.

Tet2-Deficient Hematopoietic Stem Cells Show Increased Self-Renewal Ability In Vivo

Because we have previously shown that *Tet2* deletion leads to increased replating capacity in vitro, we tested the ability of *Tet2*$^{-/-}$ cells to compete directly against wild-type counterparts in an in vivo transplantation setting. We mixed identical numbers of either *Mx1-cre*$^{+-}$ *Tet2*$^{WT/WT}$*CD45.2*$^+$ or *Mx1-cre*$^+$*Tet2*$^{f/f}$ *CD45.1*$^+$/*CD45.2*$^+$ BM from littermate mice with wild-type CD45.1$^+$ bone marrow and transplanted them in lethally irradiated CD45.1$^+$ recipients (Figure 5A). Four weeks after transplantation, equal engraftment (approximately 50:50) rates were detected in peripheral blood, and subsequently, *Tet2* deletion was induced by polyI-polyC injections. The presence of the *Tet2*-recombined allele was verified using genomic PCR of peripheral blood mononuclear cells. Chimerism was followed by FACS assessment of peripheral blood staining for CD45.1 versus CD45.2 (or CD45.1$^+$45.2$^+$). As evident from Figure 5B, upon *Tet2* deletion, *Tet2*$^{-/-}$ chimerism increased rapidly because these cells outcompeted their wild-type counterparts. Indeed, at 23 weeks after polyI-polyC deletion, more than 95% of the peripheral blood cells (both myeloid and lymphoid) were *Tet2*$^{-/-}$ (Figure 5C). To define in detail the developmental stage in which *Tet2*$^{-/-}$ cells outcompete *Tet2*-expressing cells, we have analyzed transplanted recipients 23 weeks after polyI-polyC injection. Analysis of the LT-HSC compartment indicated

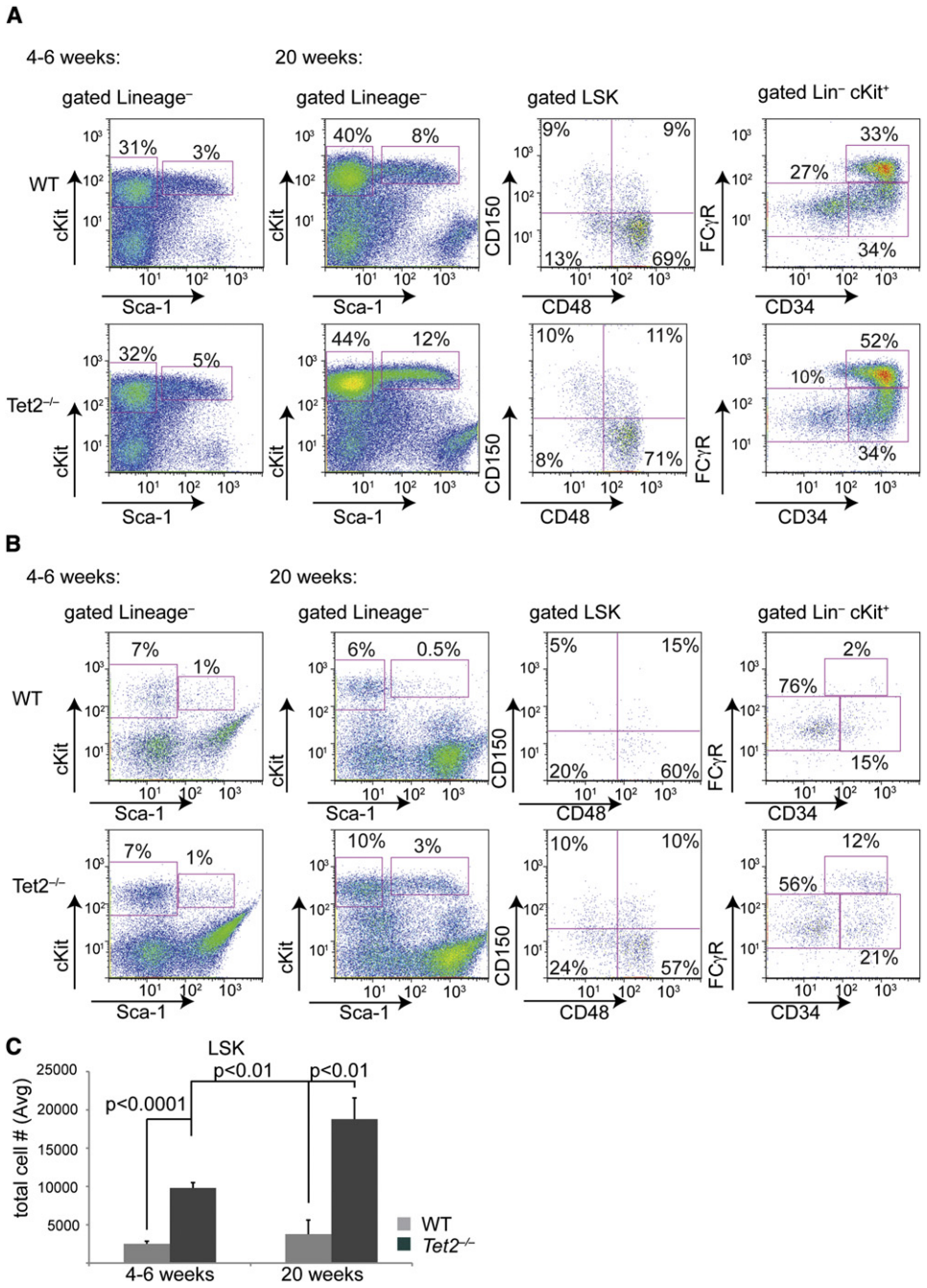

Figure 4. *Tet2* Deletion Leads to Progressive Defects in Bone Marrow and Extramedullary Hematopoiesis

(A) FACS analysis of bone marrow stem and progenitor populations of *Tet2*$^{-/-}$ (*vav-Cre*$^{+}$*Tet2*$^{f/f}$) and wild-type (*vav-Cre*$^{+}$*Tet2*$^{WT/WT}$) at two different ages (4–6 and 20 weeks). Antibody stainings are as indicated.

(B) Identical antibody labeling as in (A) but using spleen cells from *Tet2*$^{-/-}$ (*vav-Cre*$^{+}$*Tet2*$^{f/f}$) and wild-type (*vav-Cre*$^{+}$*Tet2*$^{WT/WT}$) mice.

(C) Absolute numbers of spleen LSK cells in *Tet2*$^{-/-}$ (*vav-Cre*$^{+}$*Tet2*$^{f/f}$) and wild-type (*vav-Cre*$^{+}$*Tet2*$^{WT/WT}$) mice at two different ages. p values are shown for each comparison. For all experiments shown in this figure, there are eight for each genotype. Error bars represent ± SD.

See also Figure S3.

that that the vast majority (>90%) of these cells were *Tet2*$^{-/-}$, suggesting that TET2-deficient HSC has the ability to outcompete wild-type counterparts. Once established, this bias toward the *Tet2*$^{-/-}$ cells was also observed in downstream bone marrow multipotent progenitors (MPP1,2), myeloid progenitors (CMP), bone marrow mature CD11b^{+} monocytes, and B220^{+} lymphocytes (Figures 5D and 5E). Competitive transplant studies using *VavCre*$^{+}$-*Tet2*$^{-/-}$ HSC demonstrated that TET2-deficient

cells outcompeted wild-type cells to a similar extent, further supporting our previous findings (Figure S4). These studies confirm that *Tet2* function regulates the self-renewal of adult HSC.

Tet2-Deficient Animals Develop CMML-like Disease

We next performed a detailed phenotypic analysis of $Tet2^{-/-}VavCre^{+}$ mice 20 weeks after deletion. We found that $Tet2^{-/-}$ animals, but not $Tet2^{+/+}$ littermates, were characterized by progressive leukocytosis; this was associated with neutrophilia and a marked increase in peripheral monocyte counts (Figures 6A and 6B and Table 1; Table S1). Peripheral blood analysis revealed that by week 20, approximately 70% of the $Tet2^{-/-}VavCre^{+}$ mice developed significant peripheral blood monocytosis (Figure S5). Myeloid dysplasia was apparent in both bone marrow and peripheral lymphoid tissue, as defined by myeloid left shift (presence of blasts, promyelocytes, myelocytes, or metamyelocytes). In addition, presence of hypogranular cytoplasm or abnormal segmentation of the nuclei was detected in the Tet2-deficient animals (Figures 6B and 6D; data not shown).

Moreover, $Tet2^{-/-}$ mice had significantly enlarged spleens (Figure 6C) compared to littermate controls ($p < 0.05$). Detailed pathologic analysis revealed that approximately all $Tet2^{-/-}$ mice by week 20 developed significant splenomegaly (spleen weight >250 mg), consistent with significant myeloproliferation. Histopathologic analysis revealed that $Tet2^{-/-}$ mice, but not $Tet2^{+/+}$ littermate controls, had prominent histologic evidence of disease, including significant destruction of spleen architecture, infiltration of the liver and lung, as well as bone marrow neutrophilia and monocytosis (Figure 6D). FACS analysis of the spleen of these mice revealed a significant enlargement of both the $CD11b^{+}$ and $CD11b^{+}Gr1^{+}$ populations, consistent with granulocytic and monocytic expansion (Figure 6E). Collectively, these studies demonstrate that *Tet2* loss is associated with myeloproliferation in vivo, and suggest that *TET2* mutations contribute to increased stem cell self-renewal and to progressive myeloid expansion in vivo. Although splenomegaly and leukocytosis are observed in a spectrum of myeloid malignancies, the constellation of splenomegaly, extramedullary hematopoiesis, neutrophilia, and monocytosis is most consistent with human CMML. *TET2* mutations are most commonly observed in human CMML, with somatic loss-of-function mutations in more than 40% of well-annotated CMML patient cohorts (Abdel-Wahab et al., 2009; Jankowska et al., 2009). In agreement with the murine data, detailed clinical and molecular analysis of patients with CMML revealed that patients with *TET2*-mutant CMML presented with splenomegaly, elevated peripheral blood WBC, and monocytosis (Figure S1B). Moreover, *TET2*-mutant CMML was characterized by a paucity of co-occurring cytogenetic abnormalities: 5.9% of patients with *TET2* mutant had cytogenetic abnormalities versus 61.3% of patients with *TET2*-wild-type CMML ($p = 0.018$) (Figures S1B and S1C). These studies suggested that *Tet2* deletion leads to progressive myeloproliferation in vivo with cardinal features of human CMML.

Tet2 Haploinsufficiency Is Sufficient to Initiate Aberrant Hematopoiesis In Vitro and In Vivo

Although a small subset of patients with leukemia presents with biallelic *TET2* mutations and/or deletions, the majority of patients present with monoallelic *TET2* loss (Abdel-Wahab et al., 2009; Jankowska et al., 2009). We performed DNA and cDNA sequencing of patient samples with monoallelic *TET2* mutations and demonstrated that these patients continue to express the wild-type allele (Figure S6). These data suggest the possibility that haploinsufficiency for TET2 may result in alterations in self-renewal, hematopoietic differentiation, and susceptibility to myeloid transformation. Therefore, we performed phenotypic analysis of $Tet2^{+/-}$ ($Vav\text{-}Cre^{+}Tet2^{WT/f}$) mice. We first purified $CD150^{+}$ HSC from the bone marrow of *Tet2* heterozygotes and plated them in methylcellulose cultures. Similar to $Tet2^{-/-}$ cells, $Tet2^{+/-}$ cells were able to serially replate (Figure 7A), unlike wild-type HSC that failed to generate colonies after the second plating. Likewise, $Tet2^{+/-}$ cells generated colonies with a similar immunophenotype as $Tet2^{-/-}$ cells. This was demonstrated by an immature, promyeloblastic morphology and the upregulation of the cell surface markers c-Kit, CD34, and FcγR (Figures 7B and 7C; data not shown). Furthermore, competitive reconstitution experiments, performed as described in Figure 5A, demonstrated that $Tet2^{+/-}$, but not $Tet2^{+/+}$, cells were able to outcompete wild-type counterparts, albeit with slower kinetics than $Tet2^{-/-}$ cells (Figures 7D–7H). Indeed, 23 weeks post-deletion, more than 70% of peripheral blood cells were $Tet2^{+/-}$, consistent with increased long-term self-renewal with loss of a single *Tet2* allele. Moreover, in a noncompetitive setting, 20-week-old $Vav\text{-}Cre^{+}Tet2^{WT/f}$ mice showed increased circulating monocytes (Figure 7I) and extramedullary hematopoiesis (Figures 7J and 7K), with a significant increase of both $Lineage^{neg}$ $c\text{-}Kit^{+}$ and LSK cells (Figure 7J; data not shown). These data clearly demonstrate that *Tet2* loss leads to dose-dependent effects on hematopoiesis and on myeloid transformation, and that monoallelic *TET2* loss is an important pathogenetic event in myeloid malignancies.

DISCUSSION

The identification of recurrent somatic loss-of-function mutations in *TET2* provides genetic evidence that mutational inactivation of enzymes that regulate cytosine hydroxymethylation is a common pathogenetic event in myeloid malignancies (Delhommeau et al., 2009; Ko et al., 2010; Langemeijer et al., 2009). In addition, genetic and functional studies suggest that neomorphic *IDH* mutations contribute to myeloid transformation, at least in part, by inhibiting TET enzymatic function (Figueroa et al., 2010; Xu et al., 2011). Although genetic and in vitro studies suggested a role for TET2 in regulating hematopoietic differentiation and stem/progenitor cell expansion, to our knowledge, the in vivo effects of *Tet2* loss had not previously been described. Here, we report the effects of *Tet2* loss in the hematopoietic compartment, which has allowed us to make several important observations. First, we found that *Tet2* loss leads to increased replating capacity in vitro, and that *Tet2*-deficient cells had enhanced repopulating activity in competitive reconstitution assays consistent with enhanced HSC function in vivo. Second, *Tet2* loss led to progressive myeloproliferation in vivo, with features characteristic of human CMML. In addition we found that *Tet2* haploinsufficiency confers increased self-renewal to stem/progenitor cells and to extramedullary hematopoiesis, suggesting that heterozygous loss of *TET2*, as is commonly observed in myeloid malignancies, is sufficient to contribute to myeloid transformation in vivo.

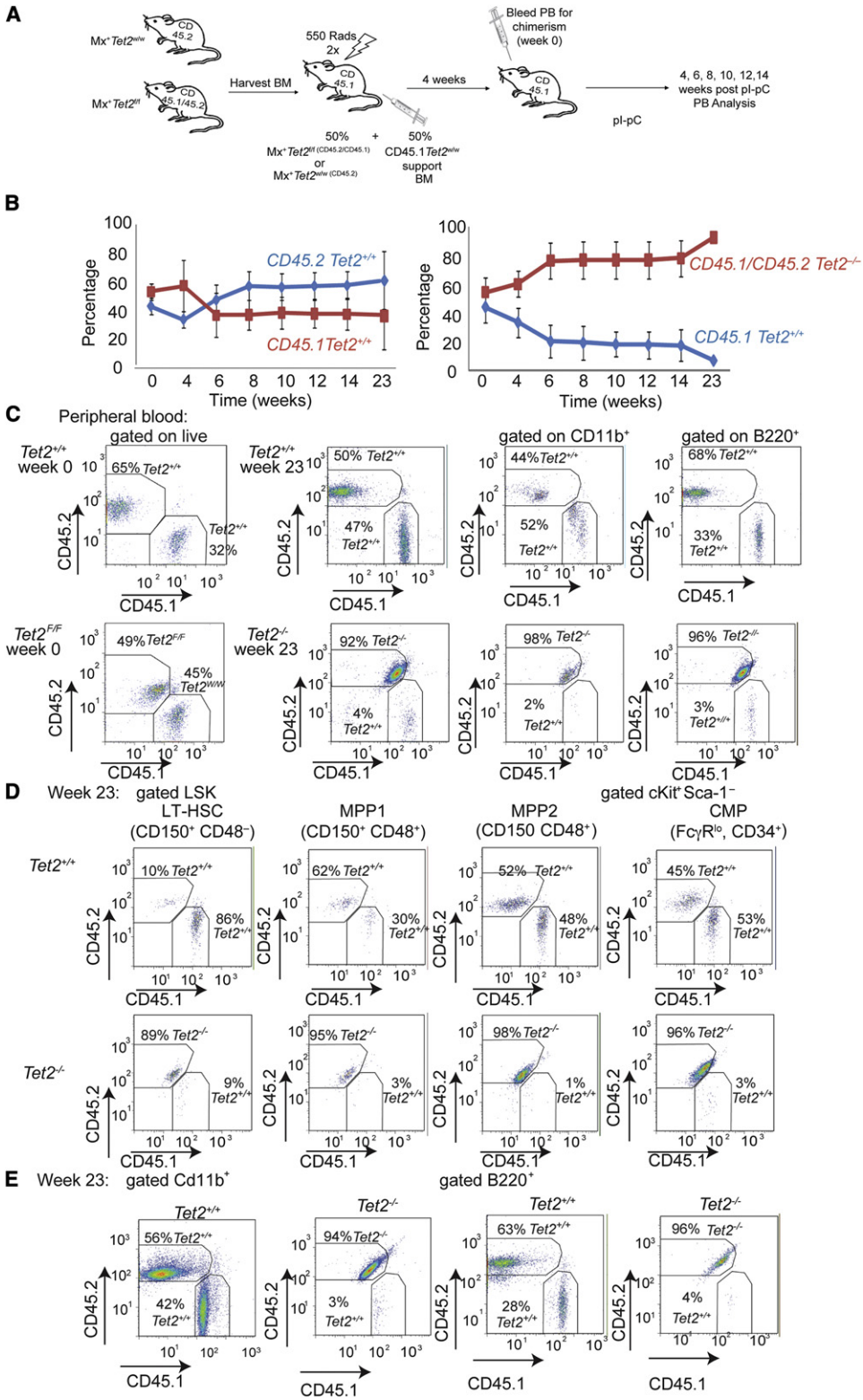

Figure 5. *Tet2*$^{-/-}$ Hematopoietic Stem Cells Show Increased Repopulating Ability Consistent with Increased Self-Renewal

(A) Schematic depiction of the competitive transplantation scheme. *Tet2*$^{-/-}$ cells are double positive for CD45.1/CD45.2 markers. *Tet2* wild-type cells are CD45.2 single positive cells.

(B) Percentage of CD45.1 versus CD45.2 total chimerism in the peripheral blood of recipient animals (n = 15 for each genotype). Time (weeks) denotes the time after the termination of polyI-polyC injections.

Our in vivo investigation of the effects of *Tet2* loss is consistent with several observations emanating from previous genetic and functional studies. The presence of *TET2* mutations in a significant proportion of patients with MPN, MDS, and AML is consistent with the notion that *TET2* loss confers increased self-renewal to stem/progenitor cells in vivo, which then leads to acquisition of mutations that direct the phenotype of *TET2*-mutant hematopoietic cells (Haeno et al., 2009; Tefferi, 2010). These data are also consistent with previous xenotransplantation studies of a small cohort of *TET2* mutant primary MPN samples that demonstrated that *TET2*-mutant MPN cells could engraft NOD-SCID mice (Delhommeau et al., 2009). In addition, genetic studies of patients with MPN that subsequently transformed to AML identified *TET2* mutations as a recurrent somatic mutation during progression from MPN to AML (Abdel-Wahab et al., 2010; Schaub et al., 2010). Our data implicate increased self-renewal as a putative mechanism of transformation by TET2 mutations, which contribute to disease initiation and progression. Our transcriptional data suggest that *Tet2* loss leads to increased expression of myeloid-specific and self-renewal gene programs. However, subsequent studies will have to functionally investigate which downstream targets of *Tet2* loss are required to confer enhanced self-renewal on stem/progenitor cells. Recent work suggested that TET proteins regulate embryonic stem cell self-renewal and differentiation (Ito et al., 2010; Koh et al., 2011). Taken together, the data suggest that *Tet2* deletion likely has effects at multiple stages in hematopoietic differentiation, and that regulation of hydroxymethylation by TET enzymes controls stem cell self-renewal and differentiation in different cellular contexts. However, to our knowledge, the exact mechanisms by which perturbations in TET enzyme function remain to be delineated. This is particularly evident given recent studies suggesting a dynamic interplay between changes in TET1-mediared hydroxymethylation and other epigenetic marks in regulating gene expression (Ficz et al., 2011; Williams et al., 2011; Wu et al., 2011), and it is likely additional alterations in the epigenetic state cooperate with TET2 mutations in malignant transformation.

In addition to effects of *Tet2* loss on self-renewal, we found that *Tet2* loss led to progressive myeloproliferation in vivo. Two recent studies used RNAi-mediated *Tet2* knockdown in vitro to suggest that TET2 depletion led to impaired hematopoietic differentiation and to preferential myeloid commitment (Figueroa et al., 2010; Ko et al., 2010). These data are consistent with our in vivo data because we observe progressive hematopoietic stem/progenitor cell expansion and myeloproliferation in vivo with *Tet2* deletion or haploinsufficiency notable for neutrophilia, monocytosis, and splenomegaly. Although these features are seen, to a varying degree, in different myeloid malignancies, they are most commonly observed in human CMML, suggesting that *Tet2* loss in the absence of other genetic lesions favors progressive myelomonocytic expansion. This is consistent with the observations that *TET2* mutations are most common in CMML (Abdel-Wahab et al., 2009; Jankowska et al., 2009) and that *TET2*-mutant CMML is characterized by fewer additional somatic cytogenetic alterations compared to *TET2*-wild-type CMML (Figures S1B and S1C). Most importantly, we demonstrate that *Tet2* haploinsufficiency is sufficient to confer increased self-renewal to stem/progenitor cells and to promote myeloproliferation in vivo. Given that the vast majority of patients with *TET2*-mutant hematopoietic malignancies retain a wild-type copy of *TET2*, our data provide functional evidence that loss of a single *TET2* allele can contribute to transformation.

Collectively, the presented data implicate *TET2* as a master regulator of normal and malignant hematopoiesis. It is likely that *TET2* has distinct roles in other hematopoietic lineages, and may contribute to transformation in lymphoid malignancies or even in epithelial tumors. These data also suggest that dysregulation of hydroxymethylation by mutations in the TET family of enzymes and by other somatic mutations may contribute to malignant transformation in other contexts. In addition it is possible that therapies that modulate hydroxymethylation levels might be of benefit in malignancies characterized by loss of TET enzyme function by inhibiting malignant stem cell self-renewal. Moreover, our studies provide insight into mechanisms of transformation by a novel class of mutations found in myeloid malignancies and in other tumors, and we predict that subsequent studies will identify additional mutations in epigenetic modifiers, which contribute to neoplasia by similar mechanisms.

EXPERIMENTAL PROCEDURES

Animals

All animals were housed at New York University School of Medicine or at Memorial Sloan-Kettering Cancer Center. All animal procedures were conducted in accordance with the Guidelines for the Care and Use of Laboratory Animals and were approved by the Institutional Animal Care and Use Committees (IACUCs) at New York University School of Medicine and Memorial Sloan-Kettering Cancer Center.

Generation of *Tet2*-Deficient Mice

The *Tet2* allele was deleted by targeting exon 3. Briefly, we have inserted two LoxP sites flanking exon 3, as well as an Frt-flanked neomycin selection cassette in the upstream intron (Figure 3A). Ten micrograms of the targeting vector was linearized by NotI and then transfected by electroporation of BAC-BA1 (C57BL/6 × 129/SvEv) hybrid embryonic stem cells. After selection with G418 antibiotic, surviving clones were expanded for PCR analysis to identify recombinant ES clones. Secondary confirmation of positive clones identified by PCR was performed by Southern blotting analysis. DNA was digested with ScaI and electrophoretically separated on a 0.8% agarose gel. After transfer to a nylon membrane, the digested DNA was hybridized with a probe targeted against the 3′ or 5′ external region. DNA from C57Bl/6 (B6), 129/SvEv (129), and BA1 (C57Bl/6 × 129/SvEv) (Hybrid) mouse strains was

(C) Representative FACS plots showing CD45.1/CD45.2 ($Tet2^{-/-}$) and CD45.2 ($Tet2^{+/+}$) stainings and chimerism in whole peripheral mononuclear cells, myeloid $CD11b^+$, and lymphoid $B220^+$ cells. Two time points (weeks 0 and 23) are shown.
(D) Representative FACS plots showing CD45.1/CD45.2 ($Tet2^{-/-}$) and CD45.2 ($Tet2^{+/+}$) stainings and chimerism within the bone marrow stem (LT-HSC) and progenitor (MPP1, MPP2, and CMP) compartments. Analysis performed at week 23 after polyI-polyC injection.
(E) Similar stainings quantifying CD45.1/CD45.2 ($Tet2^{-/-}$) and CD45.2 ($Tet2^{+/+}$) expression in bone marrow myeloid ($CD11b^+$) and lymphoid ($B220^+$) mature populations. Week 23 stainings are shown (n = 5 for each genotype). Error bars represent ± SD.
See also Figure S4.

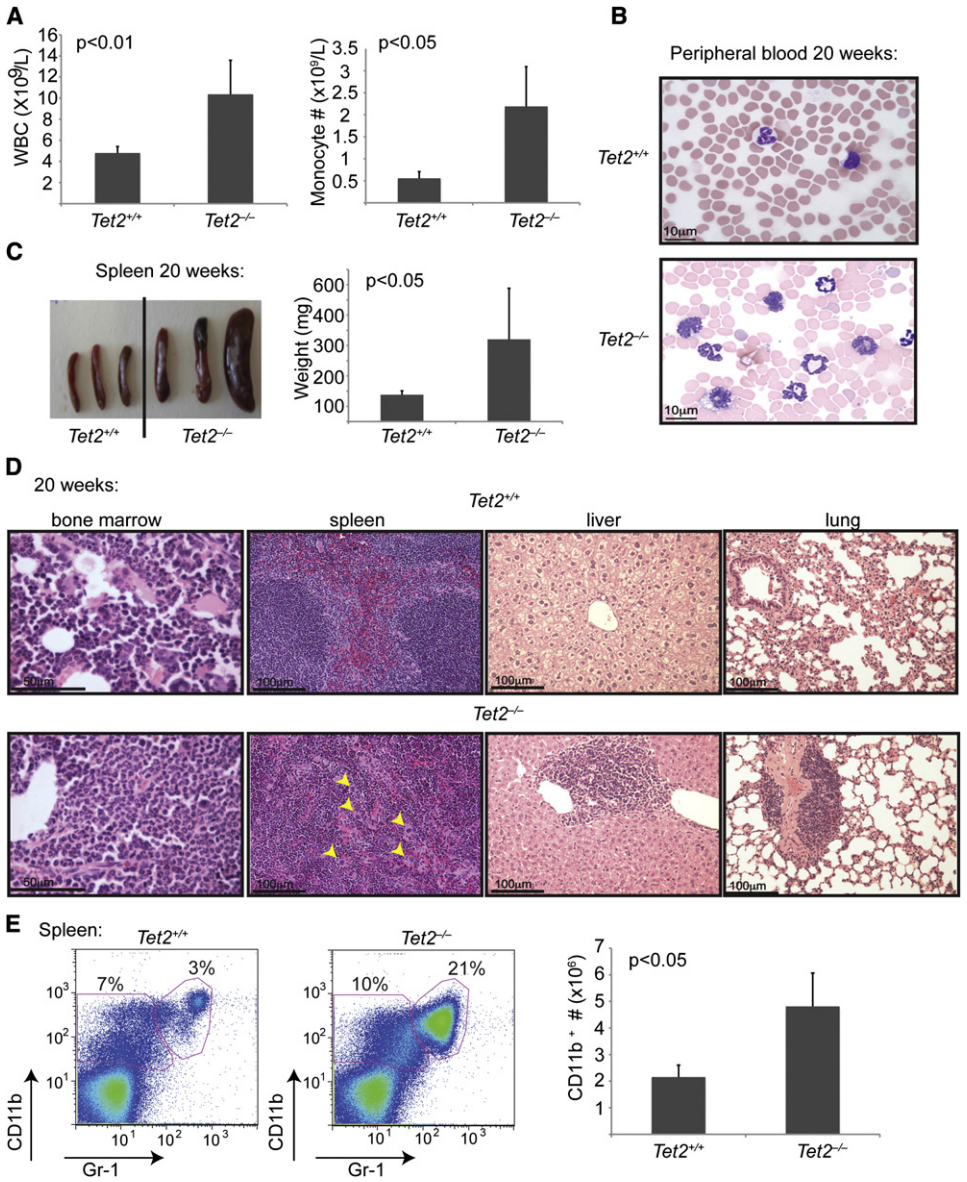

Figure 6. *Tet2*$^{-/-}$ Animals Develop Myeloid Neoplasia Reminiscent of Human CMML

(A) Left panel shows automated peripheral blood enumeration of whole blood cells (WBC). Right panel illustrates manual differential counts of neutrophils and monocytes showing blood monocytosis (n $\geq$ 3 for each genotype).

(B) Representative images of peripheral blood smears from *Tet2*$^{+/+}$ and *Tet2*$^{-/-}$ mice at 20 weeks of age (n $\geq$ 3 for each genotype).

(C) Splenomegaly in 20-week-old *Tet2*$^{-/-}$ (*Vav-Cre*$^{+}$*Tet2*$^{f/f}$) animals. Littermate wild-type (*Vav-Cre*$^{+}$*Tet2*$^{WT/WT}$) controls at 20 weeks are used (n = 5 mice).

(D) Histologic (H&E) analysis of *Tet2*$^{-/-}$ and control tissues (bone marrow, spleen, liver, and lung) is shown, illustrating disrupted spleen architecture, monocytic infiltrations in liver and lung, and bone marrow neutrophilia (n = 5 for each genotype).

(E) Left panels show FACS analysis of spleen CD11b and Gr-1-expressing populations. A representative FACS plot from each genotype is shown. Right panel illustrates total cell number of CD11b^{+} cells in the spleen of *Tet2*$^{+/+}$ and *Tet2*$^{-/-}$ mice at 20 weeks of age. Error bars represent ± SD.

See also Figure S5.

used as wild-type controls. Positive ES clones were expanded and injected into blastocysts.

The generated mice (*Tet2*$^{f/f}$) were initially crossed to a germline Flp-deleter (Jackson Laboratories), to eliminate the neomycin cassette, and subsequently to the IFNa-inducible Mx1-cre (Jackson Laboratories), the hematopoietic-specific Vav-cre, and the germline EIIa-cre (Kühn et al., 1995; Stadtfeld and Graf, 2005; Lakso et al., 1996). The Vav-Cre transgenic line was generated by the Graf laboratory (Stadtfeld and Graf, 2005) and was a gift from Virginia Shapiro (Mayo Clinic).

In Vivo Studies

Tet2 conditional and control mice received five intraperitoneal injections of poly(I:C) every other day at a dose of 20 μg/g of body weight starting at 2 weeks post-birth. For the hematopoietic-specific Vav-cre line, *Tet2*$^{f/f}$ *VavCre*$^{+}$, *Tet2*$^{f/w}$ *VavCre*$^{+}$, and *Tet2*$^{w/w}$ *VavCre*$^{+}$ mice were analyzed between 2 and 20 weeks of age. Thymus, bone marrow, spleen, and peripheral blood were analyzed by flow cytometry and formalin-fixed paraffin-embedded tissue sections stained with hematoxylin and eosin. Peripheral blood was smeared on a slide and stained using the Giemsa-Wright staining method. Tissue sections and blood

Table 1. Tet2 Deficiency Leads to Progressive Peripheral Leukocytosis

Genotype	WBC (× 10^9/l)	HCT (%)	PLT (× 10^9/l)	No.
4–6 Weeks				
Tet2$^{+/+}$	5.48 ± 1.54	40.32 ± 8.70	367 ± 66	11
Tet2$^{+/-}$	6.61 ± 1.95	49.63 ± 5.90	365 ± 59	7
Tet2$^{-/-}$	6.66 ± 2.04	50.06 ± 4.70	352 ± 85	9
20 Weeks				
Tet2$^{+/+}$	5.43 ± 1.35	46.29 ± 5.56	498 ± 171	8
Tet2$^{+/-}$	8.77 ± 1.90[a]	52.55 ± 4.42	559 ± 119	10
Tet2$^{-/-}$	10.00 ± 2.28[a]	52.45 ± 11.18	517 ± 124	13

Peripheral blood analysis (automated) at 4–6 and 20 weeks of age. See also Table S1.
[a] $p \leq 0.01$.

smears were evaluated by a hematopathologist. Deletion of the *Tet2* allele and transcript was measured by genomic PCR and quantitative real-time PCR.

Gene Expression Analysis

LSK and CMP cells were sorted from *Tet2*$^{+/+}$ *Mx-1*$^+$, *Tet*$^{-/-}$*Mx-1*$^+$ littermate mice 4 weeks post-deletion via pIC injection. Additionally, cells were obtained from serial replating of CD150$^+$-sorted Tet2-deficient cells. RNA was isolated using RNeasy RNA isolation kit (QIAGEN) according to manufacturer's protocol. A portion of total RNA (5 ng) from target cell populations was amplified and then labeled with the Ovation RNA Amplification System v2 and Ovation cDNA Biotin System (NuGEN). The resulting cDNA was hybridized to GeneChip MG 430 2.0 arrays according to the array manufacturer's recommendations (Affymetrix). The Affymetrix gene expression-profiling data were normalized using the previously published Robust Multi-array Average (RMA) algorithm using the GeneSpring GX software (Agilent, Palo Alto, CA, USA). The gene expression intensity presentation was generated with GeneSpring GX software and Multi Experiment Viewer software. Hierarchical clustering on genes and samples was performed using Euclidean distance as a metric and average linkage method (Bolstad et al., 2003).

Gene Set Enrichment Analysis

Gene Set Enrichment Analysis was performed using GSEA (Subramanian et al., 2005) http://www.broadinstitute.org/gsea/, using gene set as permutation type, 1000 permutations, and log2 ratio of classes as metric for ranking genes. Independent stem cell gene expression signatures are obtained by http://franklin.imgen.bcm.tmc.edu and Ng et al. (2009).

The "CMP signature" gene sets were generated using a systematic approach based on the comparison of gene expression arrays from wild-type LSK and wild-type GMP. Genes that were significantly modulated in CMP compared to LSK (over 1.33-fold; $p < 0.05$) were used to define CMP versus LSK_UP gene set containing upregulated genes and CMP versus LSK_DWN containing downregulated genes.

In Vitro Colony-Forming Assays

CD150$^+$ LSK as well as ckit$^+$ cells were sorted from the bone marrow of *Tet2*$^{-/-}$ *VavCre*$^+$, *Tet2*$^{+/-}$ *MxCre*$^+$, Tet2$^{-/-}$ Mx-1Cre$^+$, *Tet2*$^{+/+}$ *VavCre*$^+$, or *Tet2*$^{+/+}$ *Mx-1Cre*$^+$ mice and seeded at a density of 500 cells/replicate for the CD150$^+$ subset and 2000 cells/replicate for the cKit$^+$ subset into cytokine-supplemented methylcellulose medium (Methocult, M3434; STEMCELL Technologies). Colonies propagated in culture were scored at day 7. Representative colonies were isolated from the plate for cytospins. Remaining cells were resuspended, counted, and a portion was stained for c-kit (clone 2B8; BioLegend), and replated (4000 cells/replicate) for a total of 5 platings (7, 14, 21, 28, and 35 days). Cytospins were performed by resuspending in warm PBS and spun onto the slides at 350 × g for 5 min. Slides were air-dried and stained using the Giemsa-Wright method.

Bone Marrow Transplantation

Freshly dissected femurs and tibias were isolated from *Tet2*$^{w/w}$ *Mx-1Cre*$^+$ CD45.2$^+$, *Tet2*$^{f/w}$ *Mx-1Cre*$^+$CD45.2$^+$, or *Tet2*$^{f/f}$ *Mx-1Cre*$^+$ CD45.1$^+$/CD45.2$^+$ mice. Hence, Tet2-deficient animals are expressing both CD45.2 and CD45.1 markers, whereas *Tet2* heterozygous animals and *Tet2* wild-type control animals are expressing only the CD45.2 marker. Bone marrow was flushed with a 1 cc insulin syringe into PBS supplemented with 3% fetal bovine serum. The bone marrow was spun at 0.5 × g by centrifugation at 4°C, and red blood cells were lysed in ammonium chloride-potassium bicarbonate lysis buffer for 3 min on ice. After centrifugation, cells were resuspended in PBS plus 3% FBS, passed through a cell strainer, and counted. Finally, 0.5 × 10^6 total bone marrow cells of *Tet2*$^{w/w}$ *Mx-1Cre*$^+$ CD45.2$^+$, *Tet2*$^{f/w}$ *Mx-1Cre*$^+$CD45.2$^+$, or *Tet2*$^{f/f}$ *Mx-1Cre*$^+$ CD45.1$^+$/CD45.2$^+$ cells were mixed with 0.5 × 10^6 wild-type CD45.1$^+$-support bone marrow and transplanted via retro-orbital injection into lethally irradiated (two times 550 Gy) CD45.1$^+$ host mice. Chimerism was measured by FACS in peripheral blood at 4 weeks post-transplant (week 0, pre-polyI-polyC). Deletion of *Tet2* was initiated at this time point via five intraperitoneal injections of polyI-polyC at a dose of 20 μg/g of body weight. Chimerism for the duration of the experiment was subsequently followed via FACS in the peripheral blood every 2 weeks (week 0, 2, 4, 6, 8, 10, 12, 14, and 16 after polyI-polyC injection). Additionally, for each bleeding, whole blood cell counts were measured on a blood analyzer, and peripheral blood smears were scored. Chimerism in the bone marrow, spleen, and thymus was evaluated at 10 and 14 weeks via animal sacrifice and subsequent FACS analysis.

Mouse Bone Marrow Infections and shRNA Colony Assays

Bone marrow was harvested from the femur of wild-type C57Bl/6 mice. After red cell lysis, the bone marrow was cultured in media containing RPMI/10% FBS and IL-3 (7 ng/ml), IL-6 (10 ng/ml), and stem cell factor (10 ng/ml). The next day, cells were infected with MSCV retroviral vectors for control and *Tet2* shRNAs containing IRES GFP. Targets for shRNAs can be found in Supplemental Experimental Procedures. Cells were infected twice in the presence of polybrene and then sorted for GFP$^+$ cells 48 hr following second infection. A total of 1 × 10^4 cells was plated per well in Methocult (STEMCELL Technologies) supplemented with IL-3 (20 ng/ml), IL-6 (10 ng/ml), SCF (10 ng/ml), GMCSF (10 ng/ml), TPO (50 ng/ml), and Flt3L (100 ng/ml). Colonies were scored 14 days after seeding, recollected in PBS, and then recultured in Methocult at 1 × 10^4 cells. Tet2 knockdown was confirmed by qRT-PCR using Thermo Scientific Verso cDNA Kit and SYBR green quantification in an ABI 7500 sequence detection system.

5hmC Quantification

Genomic DNA was purified using Purgene DNA purification kit (QIAGEN). Genomic DNA was hydrolyzed and analyzed in triplicate for the relative levels of 5hmC by liquid chromatography-electrospray ionization tandem mass spectrometry (Shah et al., 2010).

Patient Samples and Sequencing

Approval was obtained from the institutional review boards of Memorial Sloan-Kettering Cancer Center, Dana-Farber Cancer Institute, and MD Anderson Cancer Center. Patients provided written informed consent in all cases at time of enrollment. DNA sequencing methods and primer sequences for TET2 have been described previously (Abdel-Wahab et al., 2009). A total of 389 AML samples were obtained at diagnosis from patients enrolled in the Eastern Cooperative Oncology Group's (ECOG) E1900 clinical trial. Samples were deidentified at the time of inclusion. A total of 354 MPN, 69 CMML, and an additional 119 AML samples were analyzed with characteristics previously described (Abdel-Wahab et al., 2009). Approval was obtained from the institutional review boards of Memorial Sloan-Kettering Cancer Center, Dana-Farber Cancer Institute, and MD Anderson Cancer Center. DNA sequencing methods and primer sequences for *TET2* have been described previously (Abdel-Wahab et al., 2009).

Human CD34$^+$ Stem Cell Isolation

Peripheral blood was collected from normal bone marrow transplant donors who underwent stem cell mobilization with GCSF. Remainder excess aliquots were used for CD34$^+$ cell isolation. CD34$^+$ HSPCs were purified by positive

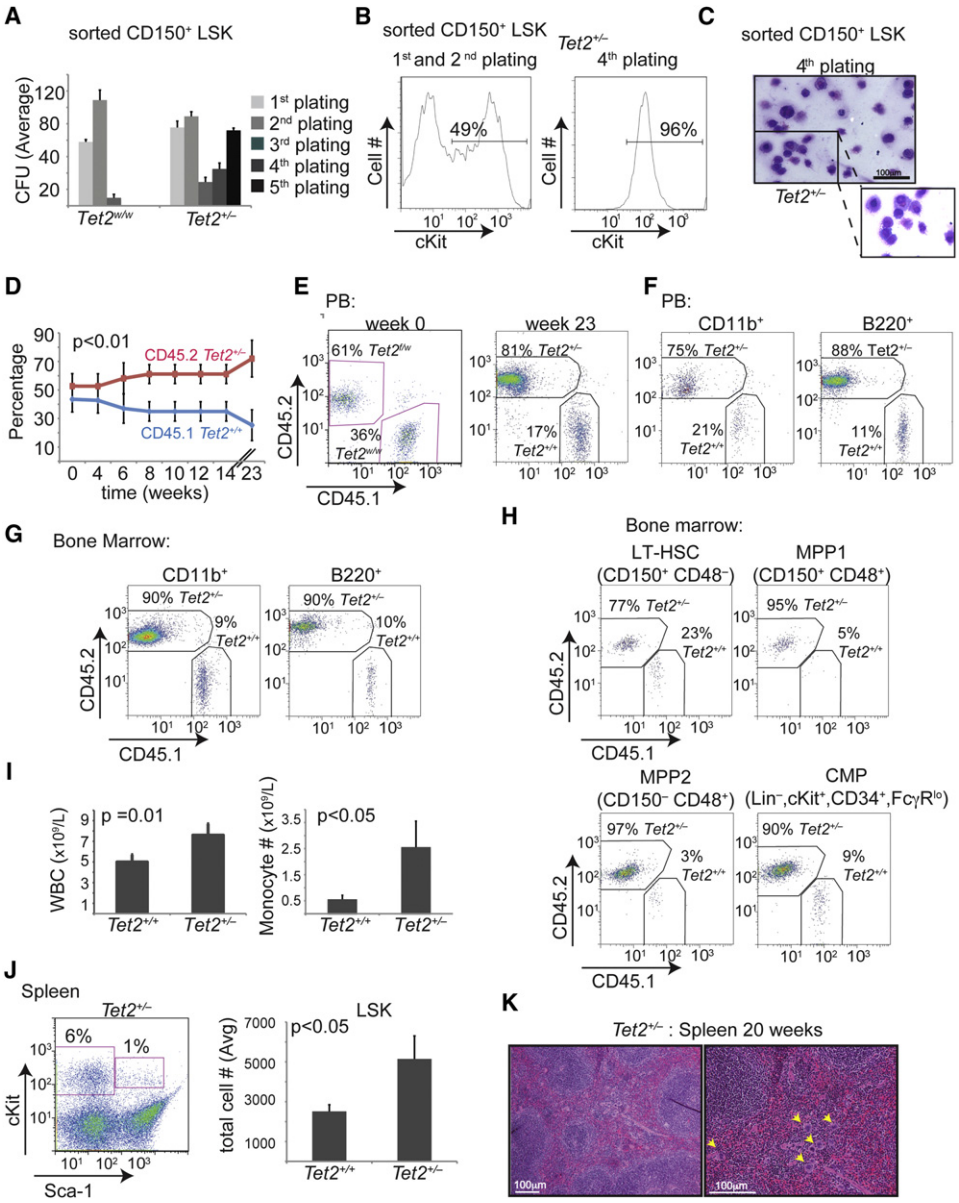

Figure 7. *Tet2* Haploinsufficiency Is Able to Initiate Aberrant In Vitro and In Vivo Hematopoiesis

(A) Methylcellulose CFU assay using LSK CD150$^+$ cells (Lin$^-$, cKit$^+$, Sca-1$^+$, CD150$^+$). An average of the absolute number of colonies is shown for sequential platings (1–5) (n = 5).

(B) Representative FACS plot of colony-forming assay showing c-Kit expression at the 2nd and 4th plating.

(C) Giemsa-Wright staining of colonies formed from *Tet2*$^{+/-}$ CD150$^+$ LSKs (*Vav-Cre*$^+$*Tet2*$^{WT/f}$). Images of cytospins are shown.

(D) Graph represents chimerism between CD45.2 (*Tet2*$^{+/-}$) and CD45.1 (*Tet2*$^{+/+}$) in the peripheral blood from a competitive transplantation assay over time (0–23 weeks). Experimental strategy is described in Figure 5A. Blue line indicates wild-type:wild-type cohorts, and red indicates *Tet2*$^{+/-}$:wild-type cohorts (n = 5 mice).

(E) Representative FACS plots showing CD45.1/CD45.2 chimerism in the peripheral blood from CD45.1 (*Tet2*$^{+/+}$) and CD45.2 (*Tet2*$^{+/-}$) cohorts before (week 0) and after deletion (23 weeks after polyI-polyC).

(F–H) Representative FACS plots showing CD45.1 (*Tet2*$^{+/+}$)/CD45.2 (*Tet2*$^{+/-}$) chimerism at 23 weeks post-deletion in myeloid and lymphoid populations in the peripheral blood (F), in the bone marrow (G), and in the bone marrow stem and progenitor cell compartment (H).

(I) Left panel shows automated peripheral blood enumeration of whole blood cells (WBC). Right panel illustrates manual differential counts of neutrophils and monocytes showing monocytosis (n $\geq$ 3 for each genotype).

(J) Representative FACS plot showing increased frequency of LSKs in the spleen of *Tet2*$^{+/-}$ mice. Right panel depicts absolute number of LSKs in the spleen of wild-type and *Tet2*$^{+/-}$ mice (n = 5 for each genotype).

(K) H&E of spleen from 20-week-old *Tet2*$^{+/-}$ mice. Error bars represent ± SD.

See also Figure S6.

selection using the Midi-magnetic-activated cell sorting LS^+ separation columns and isolation kit (Miltenyi). RNA was collected using the QIAGEN RNeasy kit.

ACCESSION NUMBERS

Microarray data can be accessed under GEO accession number GSE27816.

SUPPLEMENTAL INFORMATION

Supplemental Information includes Supplemental Experimental Procedures, six figures, and one table and can be found with this article online at doi:10.1016/j.ccr.2011.06.001.

ACKNOWLEDGMENTS

We would like to thank Hans-Guido Wendel and Dino Mavrakis for assistance with Tet2 shRNA construction. Also, we thank the NYU Genome Technology Center (supported in part by NIH/NCI P30 CA016087-30 grant) for expert assistance with microarray experiments, and the NYU Flow Cytometry facility (supported in part by NIH/NCI 5 P30CA16087-31) for expert cell sorting, the NYU Histology Core (5P30CA16087-31), and the Transgenic Mouse Core (NYU Cancer Institute Center Grant [5P30CA16087-31]). I.A. is supported by the National Institutes of Health (RO1CA133379, RO1CA105129, R21CA141399, RO1CA149655, RO1GM088847), the Leukemia & Lymphoma Society (TRP grant), the American Cancer Society (RSG0806801), the Irma T. Hirschl Trust, and the Dana Foundation. This work was supported in part by grants from the National Institutes of Health (U54CA143798-01, Physical Sciences Oncology Center) and 1R01CA138234-01, and by grants from the Starr Cancer Consortium and Howard Hughes Medical Institute to R.L.L. L.R. is supported by a NIH Ruth L. Kirchstein Award (F31-AG039991). M.E.F. is funded by a Leukemia and Lymphoma Society Special Fellow award. A.M. is funded by a Leukemia and Lymphoma Society SCOR and TRP award, and is a Burroughs Wellcome Clinical Translational Scholar and Scholar of the Leukemia and Lymphoma Society. A.M. and M.E.F. are also supported by the Sackler Center for Biomedical and Physical Sciences. L.A.G. was supported by the NIH Grants CA129831 and CA129831-03S1. X.Z. and S.D.N. are supported by a Leukemia and Lymphoma Society SCOR award and FP by an American Italian Cancer Foundation award. R.L.L. is a Geoffrey Beene Junior Faculty Chair at Memorial Sloan-Kettering Cancer Center. I.A. is a Howard Hughes Medical Institute Early Career Scientist.

Received: March 4, 2011
Revised: May 3, 2011
Accepted: June 6, 2011
Published online: June 30, 2011

REFERENCES

Abdel-Wahab, O., and Levine, R.L. (2010). *EZH2* mutations: mutating the epigenetic machinery in myeloid malignancies. Cancer Cell *18*, 105–107.

Abdel-Wahab, O., Mullally, A., Hedvat, C., Garcia-Manero, G., Patel, J., Wadleigh, M., Malinge, S., Yao, J., Kilpivaara, O., Bhat, R., et al. (2009). Genetic characterization of TET1, TET2, and TET3 alterations in myeloid malignancies. Blood *114*, 144–147.

Abdel-Wahab, O., Manshouri, T., Patel, J., Harris, K., Yao, J., Hedvat, C., Heguy, A., Bueso-Ramos, C., Kantarjian, H., Levine, R.L., and Verstovsek, S. (2010). Genetic analysis of transforming events that convert chronic myeloproliferative neoplasms to leukemias. Cancer Res. *70*, 447–452.

Bolstad, B.M., Irizarry, R.A., Astrand, M., and Speed, T.P. (2003). A comparison of normalization methods for high density oligonucleotide array data based on variance and bias. Bioinformatics *19*, 185–193.

Dang, L., White, D.W., Gross, S., Bennett, B.D., Bittinger, M.A., Driggers, E.M., Fantin, V.R., Jang, H.G., Jin, S., Keenan, M.C., et al. (2009). Cancer-associated IDH1 mutations produce 2-hydroxyglutarate. Nature *462*, 739–744.

Delhommeau, F., Dupont, S., Della Valle, V., James, C., Trannoy, S., Massé, A., Kosmider, O., Le Couedic, J.P., Robert, F., Alberdi, A., et al. (2009). Mutation in TET2 in myeloid cancers. N. Engl. J. Med. *360*, 2289–2301.

Dorrance, A.M., Liu, S., Yuan, W., Becknell, B., Arnoczky, K.J., Guimond, M., Strout, M.P., Feng, L., Nakamura, T., Yu, L., et al. (2006). Mll partial tandem duplication induces aberrant Hox expression in vivo via specific epigenetic alterations. J. Clin. Invest. *116*, 2707–2716.

Ernst, T., Chase, A.J., Score, J., Hidalgo-Curtis, C.E., Bryant, C., Jones, A.V., Waghorn, K., Zoi, K., Ross, F.M., Reiter, A., et al. (2010). Inactivating mutations of the histone methyltransferase gene EZH2 in myeloid disorders. Nat. Genet. *42*, 722–726.

Ficz, G., Branco, M.R., Seisenberger, S., Santos, F., Krueger, F., Hore, T.A., Marques, C.J., Andrews, S., and Reik, W. (2011). Dynamic regulation of 5-hydroxymethylcytosine in mouse ES cells and during differentiation. Nature *473*, 398–402.

Figueroa, M.E., Abdel-Wahab, O., Lu, C., Ward, P.S., Patel, J., Shih, A., Li, Y., Bhagwat, N., Vasanthakumar, A., Fernandez, H.F., et al. (2010). Leukemic IDH1 and IDH2 mutations result in a hypermethylation phenotype, disrupt TET2 function, and impair hematopoietic differentiation. Cancer Cell *18*, 553–567.

Gilliland, D.G., and Griffin, J.D. (2002). The roles of FLT3 in hematopoiesis and leukemia. Blood *100*, 1532–1542.

Haeno, H., Levine, R.L., Gilliland, D.G., and Michor, F. (2009). A progenitor cell origin of myeloid malignancies. Proc. Natl. Acad. Sci. USA *106*, 16616–16621.

Ito, S., D'Alessio, A.C., Taranova, O.V., Hong, K., Sowers, L.C., and Zhang, Y. (2010). Role of Tet proteins in 5mC to 5hmC conversion, ES-cell self-renewal and inner cell mass specification. Nature *466*, 1129–1133.

Jankowska, A.M., Szpurka, H., Tiu, R.V., Makishima, H., Afable, M., Huh, J., O'Keefe, C.L., Ganetzky, R., McDevitt, M.A., and Maciejewski, J.P. (2009). Loss of heterozygosity 4q24 and TET2 mutations associated with myelodysplastic/myeloproliferative neoplasms. Blood *113*, 6403–6410.

Ko, M., Huang, Y., Jankowska, A.M., Pape, U.J., Tahiliani, M., Bandukwala, H.S., An, J., Lamperti, E.D., Koh, K.P., Ganetzky, R., et al. (2010). Impaired hydroxylation of 5-methylcytosine in myeloid cancers with mutant TET2. Nature *468*, 839–843.

Koh, K.P., Yabuuchi, A., Rao, S., Huang, Y., Cunniff, K., Nardone, J., Laiho, A., Tahiliani, M., Sommer, C.A., Mostoslavsky, G., et al. (2011). Tet1 and Tet2 regulate 5-hydroxymethylcytosine production and cell lineage specification in mouse embryonic stem cells. Cell Stem Cell *8*, 200–213.

Krivtsov, A.V., Feng, Z., Lemieux, M.E., Faber, J., Vempati, S., Sinha, A.U., Xia, X., Jesneck, J., Bracken, A.P., Silverman, L.B., et al. (2008). H3K79 methylation profiles define murine and human MLL-AF4 leukemias. Cancer Cell *14*, 355–368.

Kühn, R., Schwenk, F., Aguet, M., and Rajewsky, K. (1995). Inducible gene targeting in mice. Science *269*, 1427–1429.

Lakso, M., Pichel, J.G., Gorman, J.R., Sauer, B., Okamoto, Y., Lee, E., Alt, F.W., and Westphal, H. (1996). Efficient in vivo manipulation of mouse genomic sequences at the zygote stage. Proc. Natl. Acad. Sci. USA *93*, 5860–5865.

Langemeijer, S.M., Kuiper, R.P., Berends, M., Knops, R., Aslanyan, M.G., Massop, M., Stevens-Linders, E., van Hoogen, P., van Kessel, A.G., Raymakers, R.A., et al. (2009). Acquired mutations in TET2 are common in myelodysplastic syndromes. Nat. Genet. *41*, 838–842.

Ley, T.J., Ding, L., Walter, M.J., McLellan, M.D., Lamprecht, T., Larson, D.E., Kandoth, C., Payton, J.E., Baty, J., Welch, J., et al. (2010). DNMT3A mutations in acute myeloid leukemia. N. Engl. J. Med. *363*, 2424–2433.

Mardis, E.R., Ding, L., Dooling, D.J., Larson, D.E., McLellan, M.D., Chen, K., Koboldt, D.C., Fulton, R.S., Delehaunty, K.D., McGrath, S.D., et al. (2009). Recurring mutations found by sequencing an acute myeloid leukemia genome. N. Engl. J. Med. *361*, 1058–1066.

Metzeler, K.H., Maharry, K., Radmacher, M.D., Mrozek, K., Margeson, D., Becker, H., Curfman, J., Holland, K.B., Schwind, S., Whitman, S.P., et al. (2011). TET2 mutations improve the new European LeukemiaNet risk classification of acute myeloid leukemia: a Cancer and Leukemia Group B study. J. Clin. Oncol. *29*, 1373–1381.

Morin, R.D., Johnson, N.A., Severson, T.M., Mungall, A.J., An, J.H., Goya, R., Paul, J.E., Boyle, M., Woolcock, B.W., Kuchenbauer, F., et al. (2010). Somatic mutations altering EZH2 (Tyr641) in follicular and diffuse large B-cell lymphomas of germinal-center origin. Nat. Genet. *42*, 181–185.

Ng, S.Y., Yoshida, T., Zhang, J., and Georgopoulos, K. (2009). Genome-wide lineage-specific transcriptional networks underscore Ikaros-dependent lymphoid priming in hematopoietic stem cells. Immunity *30*, 493–507.

Nikoloski, G., Langemeijer, S.M., Kuiper, R.P., Knops, R., Massop, M., Tönnissen, E.R., van der Heijden, A., Scheele, T.N., Vandenberghe, P., de Witte, T., et al. (2010). Somatic mutations of the histone methyltransferase gene EZH2 in myelodysplastic syndromes. Nat. Genet. *42*, 665–667.

Parsons, D.W., Jones, S., Zhang, X., Lin, J.C., Leary, R.J., Angenendt, P., Mankoo, P., Carter, H., Siu, I.M., Gallia, G.L., et al. (2008). An integrated genomic analysis of human glioblastoma multiforme. Science *321*, 1807–1812.

Schaub, F.X., Looser, R., Li, S., Hao-Shen, H., Lehmann, T., Tichelli, A., and Skoda, R.C. (2010). Clonal analysis of TET2 and JAK2 mutations suggests that TET2 can be a late event in the progression of myeloproliferative neoplasms. Blood *115*, 2003–2007.

Shah, M.Y., Vasanthakumar, A., Barnes, N.Y., Figueroa, M.E., Kamp, A., Hendrick, C., Ostler, K.R., Davis, E.M., Lin, S., Anastasi, J., et al. (2010). DNMT3B7, a truncated DNMT3B isoform expressed in human tumors, disrupts embryonic development and accelerates lymphomagenesis. Cancer Res. *70*, 5840–5850.

Stadtfeld, M., and Graf, T. (2005). Assessing the role of hematopoietic plasticity for endothelial and hepatocyte development by non-invasive lineage tracing. Development *132*, 203–213.

Subramanian, A., Tamayo, P., Mootha, V.K., Mukherjee, S., Ebert, B.L., Gillette, M.A., Paulovich, A., Pomeroy, S.L., Golub, T.R., Lander, E.S., and Mesirov, J.P. (2005). Gene set enrichment analysis: a knowledge-based approach for interpreting genome-wide expression profiles. Proc. Natl. Acad. Sci. USA *102*, 15545–15550.

Tahiliani, M., Koh, K.P., Shen, Y., Pastor, W.A., Bandukwala, H., Brudno, Y., Agarwal, S., Iyer, L.M., Liu, D.R., Aravind, L., and Rao, A. (2009). Conversion of 5-methylcytosine to 5-hydroxymethylcytosine in mammalian DNA by MLL partner TET1. Science *324*, 930–935.

Tefferi, A. (2010). Novel mutations and their functional and clinical relevance in myeloproliferative neoplasms: JAK2, MPL, TET2, ASXL1, CBL, IDH and IKZF1. Leukemia *24*, 1128–1138.

van Haaften, G., Dalgliesh, G.L., Davies, H., Chen, L., Bignell, G., Greenman, C., Edkins, S., Hardy, C., O'Meara, S., Teague, J., et al. (2009). Somatic mutations of the histone H3K27 demethylase gene UTX in human cancer. Nat. Genet. *41*, 521–523.

Varela, I., Tarpey, P., Raine, K., Huang, D., Ong, C.K., Stephens, P., Davies, H., Jones, D., Lin, M.L., Teague, J., et al. (2011). Exome sequencing identifies frequent mutation of the SWI/SNF complex gene PBRM1 in renal carcinoma. Nature *469*, 539–542.

Ward, P.S., Patel, J., Wise, D.R., Abdel-Wahab, O., Bennett, B.D., Coller, H.A., Cross, J.R., Fantin, V.R., Hedvat, C.V., Perl, A.E., et al. (2010). The common feature of leukemia-associated IDH1 and IDH2 mutations is a neomorphic enzyme activity converting alpha-ketoglutarate to 2-hydroxyglutarate. Cancer Cell *17*, 225–234.

Williams, K., Christensen, J., Pedersen, M.T., Johansen, J.V., Cloos, P.A., Rappsilber, J., and Helin, K. (2011). TET1 and hydroxymethylcytosine in transcription and DNA methylation fidelity. Nature *473*, 343–348.

Wu, H., D'Alessio, A.C., Ito, S., Xia, K., Wang, Z., Cui, K., Zhao, K., Eve Sun, Y., and Zhang, Y. (2011). Dual functions of Tet1 in transcriptional regulation in mouse embryonic stem cells. Nature *473*, 389–393.

Xu, W., Yang, H., Liu, Y., Yang, Y., Wang, P., Kim, S.H., Ito, S., Yang, C., Wang, P., Xiao, M.T., et al. (2011). Oncometabolite 2-hydroxyglutarate is a competitive inhibitor of α-ketoglutarate-dependent dioxygenases. Cancer Cell *19*, 17–30.

Yamashita, Y., Yuan, J., Suetake, I., Suzuki, H., Ishikawa, Y., Choi, Y.L., Ueno, T., Soda, M., Hamada, T., Haruta, H., et al. (2010). Array-based genomic resequencing of human leukemia. Oncogene *29*, 3723–3731.

Yan, H., Parsons, D.W., Jin, G., McLendon, R., Rasheed, B.A., Yuan, W., Kos, I., Batinic-Haberle, I., Jones, S., Riggins, G.J., et al. (2009). IDH1 and IDH2 mutations in gliomas. N. Engl. J. Med. *360*, 765–773.